International Journal of Nanomedicine

Dovepress
open access to scientific and medical research

Open Access Full Text Article

ORIGINAL RESEARCH

CD133-Targeted Hybrid Nanovesicles for Fluorescent/Ultrasonic Imaging-Guided HIFU Pancreatic Cancer Therapy

Rui Wang[1,*], Yijing Yao[1,2,*], Yihui Gao[1], Mengyao Liu[1], Qian Yu[3], Xuejiao Song[4], Xiao Han[5], Dechao Niu[6], Lixin Jiang[1,2]

[1]Department of Ultrasound, Renji Hospital, School of Medicine, Shanghai Jiaotong University, Shanghai, 200127, People's Republic of China; [2]Shanghai Institute of Ultrasound in Medicine, Shanghai, 200233, People's Republic of China; [3]Department of Ultrasonography, Shanghai Jiao Tong University Affiliated No. 6 Hospital, Shanghai, 200233, People's Republic of China; [4]School of Physical and Mathematical Sciences, Nanjing Tech University (NanjingTech), Nanjing, 211800, People's Republic of China; [5]Institute of Functional Nano & Soft Materials (FUNSOM), Jiangsu Key Laboratory for Carbon-Based Functional Materials and Devices, Soochow University, Suzhou, Jiangsu, 215123, People's Republic of China; [6]Lab of Low-Dimensional Materials Chemistry, Key Laboratory for Ultrafine Materials of Ministry of Education, School of Materials Science and Engineering, East China University of Science and Technology, Shanghai, 200237, People's Republic of China

*These authors contributed equally to this work

Correspondence: Lixin Jiang; Dechao Niu, Email jinger_28@sina.com; dcniu@ecust.edu.cn

Background: Pancreatic cancer is regarded as one of the most lethal types of tumor in the world, and optional way to treat the tumor are urgently needed. Cancer stem cells (CSCs) play a key role in the occurrence and development of pancreatic tumors. CD133 is a specific antigen for targeting the pancreatic CSCs subpopulation. Previous studies have shown that CSC-targeted therapy is effective in inhibiting tumorigenesis and transmission. However, CD133 targeted therapy combined with HIFU for pancreatic cancer is absent.

Purpose: To improve therapeutic efficiency and minimize side effects, we carry a potent combination of CSCs antibody with synergist by an effective and visualized delivery nanocarrier to pancreatic cancer.

Materials and Methods: Multifunctional CD133-targeted nanovesicles (CD133-grafted Cy5.5/PFOB@P-HVs) with encapsulated perfluorooctyl bromide (PFOB) in a 3-mercaptopropyltrimethoxysilane (MPTMS) shell modified with poly ethylene glycol (PEG) and superficially modified with CD133 and Cy 5.5 were constructed following the prescribed order. The nanovesicles were characterized for the biological and chemical characteristics feature. We explored the specific targeting capacity in vitro and the therapeutic effect in vivo.

Results: The in vitro targeting experiment and in vivo FL and ultrasonic experiments showed the aggregation of CD133-grafted Cy5.5/PFOB@P-HVs around CSCs. In vivo FL imaging experiments demonstrated that the nanovesicles assemble for the highest concentration in the tumor at 24 h after administration. Under HIFU irradiation, the synergistic efficacy of the combination of the CD133-targeting carrier and HIFU for tumor treatment was obvious.

Conclusion: CD133-grafted Cy5.5/PFOB@P-HVs combined with HIFU irradiation could enhance the tumor treatment effect not only by improving the delivery of nanovesicles but also by enhancing the HIFU thermal and mechanical effects in the tumor microenvironment, which is a highly effective targeted therapy for treating pancreatic cancer.

Keywords: multifunctional nanovesicles, cancer stem cells, high-intensity focused ultrasound, in vivo fluorescent imaging, ultrasonic imaging

Introduction

Pancreatic tumor is one of the most malignant forms of cancer, having a 5-year survival rate of as low as 8% in the United States,[1] and causing approximately 250,000 deaths worldwide.[2] Pancreatic cancer is thought to be incurable at present, with a high recurrence and metastasis rate in post-operation and with minimal responsiveness to chemotherapy.[3] The mechanism of pancreatic cancer development has not been clarified yet, and some recent studies suggest that a subset of cells, known as cancer stem cells (CSCs) may be related to tumor recurrence, high lethality, and chemotherapy resistance.[4–6] CD133,

Received: 17 November 2022
Accepted: 16 April 2023
Published: 12 May 2023

ALDH, and CD44CD24ESA are key molecular biomarkers for identifying pancreatic CSCs, and their glycoprotein expression is used to enrich tumor initiating cells and is closely associated with resistance to chemotherapy and radiation.[7] CD133 has been used as a marker for stem cells (human hematopoietic stem cell,[8] endothelial precursor cells,[9] prostate epithelial stem cells[10]). It was the first well-characterized CSC surface marker[11] and later identified as a CSCs marker in breast CSCs,[12] colon CSCs,[13,14] hepatic CSCs,[15,16] prostate CSCs[17] and brain CSCs.[11,18] It was the first identified CSCs marker in pancreatic cancer.[7] CD133 is associated with pancreatic cancer initiating and recurring activity. Herman[6] detected that as few as 500 CD133+ isolated pancreatic cancer cells were capable of developing orthotopic pancreatic tumor formation in nude mice. Emerging CSCs-targeting nanovesicles may be an efficient tool for tracing and eliminating CSCs.[19] CD133 targeted anticancer drug has been developed for breast cancer,[20] hepatic cancer,[21–23]prostate cancer[24] and glioma.[25,26] The above study confirmed that CD133 targeted treatment improves the cancer diagnosis and therapy efficiency. However, the CD133 targeted specific nanovesicles study for pancreatic cancer is absent. Our study aimed to develop CD133 targeted nanovesicles and explored the combined therapy efficiency.

High-intensity focused ultrasound (HIFU) is an emerging technique that is regarded as a minimally invasive treatment for tumors compared to surgical resection, chemotherapy, and radiotherapy.[27–31] To improve the precision of imaging-guided HIFU therapy and reduce the HIFU dose to avoid side effects, HIFU synergistic agents (SAs), especially targeted nanovesicles, can be transported to the tumor site idiopathically through blood circulation.[32,33] Perfluorooctyl bromide (PFOB) is one of the most common HIFU SAs because of its property of intensifying the activation effect of HIFU.[34–37] Selecting the appropriate carrier, such as poly(lactic-co-glycolic acid), mesoporous silica, and organosilica, is very important.[38–43] 3-mercaptopropyltrimethoxysilane (MPTMS) is an emerging organosilica that is metabolized and expelled by the liver via excretions.[42–48]

Herein, we design the multifunctional and targeted organic/inorganic hybrid vesicles for the treatment of pancreatic cancer via HIFU therapy. Nanovesicles formulated using the MPTMS polymer and surface decorated with anti-CD133 antibodies were developed for targeting pancreatic CSCs. As shown in Scheme 1, the nanoparticles were characterized for their effectiveness against CSCs through in vitro experiments and their ability to inhibit tumor growth was certified in a pancreatic cancer mouse model. Thus, the novel multifunctional and CD133-targeted nanovesicles (CD133-grafted Cy5.5/PFOB@P-HVs) contribute to improving the therapeutic efficacy against pancreatic cancer.

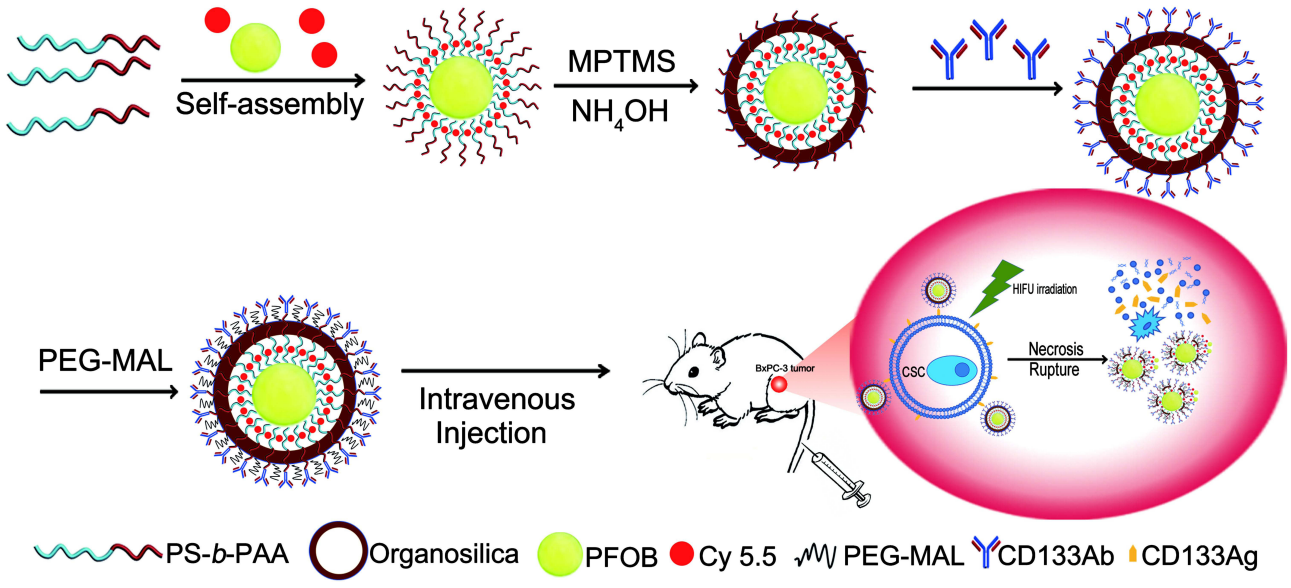

Scheme 1 Schematic illustration of nanovesicles synthesis and the antitumor mechanism triggered by HIFU and CD133-grafted Cy5.5/PFOB@P-HVs.

Materials and Methods

Materials

3-mercaptopropyltrimethoxysilane (MPTMS) was obtained from ABCR GmbH &Co KG (Karlsruhe, Germany). Tetrahydrofuran (THF) was purchased from Shanghai Lingfeng Chemical Reagent Co. Ltd. (Shanghai, China). mPEG-MAL was purchased from Shanghai Yubo Biology Co. Ltd. (Shanghai, China). Ammonia solution (28%) was obtained from Shanghai Yubo Biology Co. Ltd. (Shanghai, China). PFOB was purchased from Elf Atochem Chemical Reagent Co. Ltd. (Germany). PS_{100}-*b*-PAA_{16}, an amphiphilic block copolymer, was synthesized via traditional atom transfer radical polymerization, as described previously.[39] Cy5.5 dye mono-reactive NHS esters (Cy5.5 NHS-ester) was purchased by Shanghai Yudole Biotechnology Co. LTD (Shanghai, China). CD133 antibodies (AC 141) were obtained from Miltenyi Biotec GmbH (Auburn, CA) and IgG isotype control antibodies were purchased from Shanghai Yudole Biotechnology Co. LTD (Shanghai, China). Distilled water was used in all manipulation.

Synthesis of Fluorescent Ultrasonic Nanovesicles

For this experiment, 10 mg of PS_{100}-*b*-PAA_{16} and 0.3 mg of Cy5.5 were dissolved in 4 mL of THF. Later, 60 μL of PFOB and 0.3 mg of Cy5.5 were mixed into the above solution. Subsequently, the solution was poured into 40 mL of distilled water and mixed at atmospheric temperature for about 5 minutes. Then, ammonia water (1 mL, 28%) was quickly put into the micellar mixture when the pH reached 12. In order to maintain the micellar structure, 75 μL of MPTMS was poured into this initial emulsion. The copolymer solution was mechanically stirred at atmospheric temperature for 24 hours to produce the mixture. Subsequently, dialyzed separately for 24 h. Two mg each of EDC and NHS were poured into the above solution, and mechanical stirring was performed at atmospheric temperature for 4 h. Then, the solution was centrifuged at 13,000 rpm for 30 min. The sediment was redistributed with 20 mL of autoclaved deionized water, and 0.1 mg of CD133/lgG antibodies were added. The normal temperature was set as 4°C, and stirring was performed for 2 h. Then, the final solution was mechanically mixed at room temperature for 2 h and allowed to stand in one night. PEG-MAL (30 mg) was added to maintain the micellar structural stability, and then, the solution was centrifuged at 13,000 rpm for 30 min. The sample (CD133-grafted Cy5.5/PFOB@P-HVs and IgG-grafted Cy5.5/PFOB@P-HVs) was re-dispersed in phosphate-buffered saline (PBS) for further experiments.

Characterization

The morphological characterization of nanovesicles was performed via scanning electron microscopy (SEM, FEI Magellan 400L system, USA) and transmission electron microscopy (TEM, JEM 2100F, Japan). The mean diameters, size distributions, and zeta potentials of the samples were measured using a particle size analyzer (Zeta SIZER, Malvern, USA). The fluorescence intensity was studied using a confocal laser scanning microscopy (LSM710, Carl Zeiss, Oberkochen, Germany). The emission wavelength of the nanovesicles after synthesis was measured using a fluorospectro photometer (FL8500, PerkinElmer, USA). The PFOB encapsulation rate was analyzed by the proportion of thermal analyzer (TGA4000, PerkinElmer, USA). Inductively coupled plasma-atomic emission spectroscopy (ICP-AES) was administered on an ICP emission spectrometer (Optima 8300, PerkinElmer, US). A HIFU therapy system (HY2980, Wuxi Haiying Technology Co. Ltd, Wuxi, China) was used to carry out the nude mouse experiments.

Morphology Changes in Nanovesicles Under HIFU Irradiation

Nanovesicles solutions (5 mg/mL) were added into five samples and treated with different doses of HIFU irradiation. A small animal HIFU therapy system (Wuxi Haiying Technology, China, HY2980) was used to irradiate the solutions at 10W for 5min, respectively. After HIFU treatment, the meanwhile surface morphological feature of the particles was observed using TEM.

Cell Culture

Three human pancreatic cancer cell lines, namely, BxPC-3, PANC-1, and SW1990, were obtained from the cell library of the Chinese Academy of Sciences (Shanghai, China), and cultured in RPMI-1640 medium, Dulbecco's modified eagle

medium (DMEM), and Leibovitz L 15 medium (Gibco, USA), respectively. The culture solution was favored with fetal bovine serum (FBS, 10%, Gibco, USA), streptomycin (100 U/mL), and penicillin (100 U/mL). The cells were incubated at 37°C under an atmosphere of 5% CO_2.

In vitro Cytotoxicity and in vivo Biosafety Studies

The cytotoxicity was evaluated using the CCK-8 assay. The BxPC-3 cell lines were cultured in DMEM containing 10% FBS (approximately 5000 cells/well) and incubated at 37°C under 5% CO_2. The groups were divided into six groups: saline, IgG-grafted Cy5.5@P-HVs, CD133-grafted Cy5.5@P-HVs, IgG-grafted Cy5.5@P-HVs+HIFU, CD133-grafted Cy5.5@P-HVs+HIFU, CD133-grafted Cy5.5/PFOB@P-HVs+HIFU. The cells were cultured in 96-well panels for 24 hours, and then co-cultured with above groups individually at concentrations of 0, 5, 10, 15, and 20 mg/mL for 24 h or 48 h. Later, 10 μL of CCK-8 solution (Beyotime, China) was added to every well. After cocultivation for 4 h, a multi-functional ELIASA was used to measure the solution absorbance in each sample at 450 nm. Each detection value was taken as the mean value of six samples, and 100% viability was obtained from the control group. Every result was repeated for three times.

To evaluate the cytotoxicity of CD133-grafted Cy5.5/PFOB@P-HVs ex vitro, twenty-five tumor-bearing nude mouse were classed for five groups (n = 5) at random. After adaptive feeding for one week, five groups individually were intravenously administered into mice. The body weight of mice was recorded every two days. After 14-day observation, the blood and main organs (heart, liver, spleen, lung, and kidney), of mice were collected for blood routine indexes, biochemical analysis and H&E staining.

Flow Cytometry Analysis of Three Pancreatic Cancer Cell Lines

We evaluated the CD133 expression levels in three pancreatic cancer cell lines, namely, BxPC-3, PANC-1, and SW1990, using flow cytometry. The cells were trypsinized from the culture plate using 0.25% trypsin, washed with PBS, and suspended at 1×10^6 cells/mL in a culture medium. FcR Blocking Reagent (Miltenyi Biotec, Germany) was added and the cells were re-suspended in buffer. Anti-human CD133-antibody conjugated with fluorescent R-phycoerythrin (CD133 mouse mAb, Miltenyi Biotec, Germany) was used to label the cells. The cell solution was mixed well and incubated for 10 min in the dark in a refrigerator (2−8°C). The cells were washed by adding ice buffer and then centrifuged, and the supernatant was aspirated completely. The cell pellets were resuspended in a suitable amount of ice buffer for analysis by flow cytometry (FACS Calibur, Beckman Dickson). The tests were conducted in triplicate.

Validation of the Targeting Capacity of Nanovesicles ex vivo at the Cell Level

To test the ex vivo targeting capacity of CD133-grafted Cy5.5/PFOB@P-HVs with CD133-positive pancreatic CSCs, CD133-positive CSCs and CD133-negative pancreatic cancer cells were first separated from general BxPC-3 pancreatic cancer cells by magnetic activated cell sorting (MACS). The suspended BxPC-3 CSCs were fixed with 4% paraformaldehyde in PBS for 15 min. The CSCs and non-CSCs were treated with CD133-grafted Cy5.5/PFOB@P-HVs (with 3.8 μM of Cy5.5) individually for 4 h, and rinsed with PBS thrice to eliminate unbounded CD133-grafted Cy5.5/PFOB@P-HVs. The cell nuclei were stained with DAPI (Beyotime, China). The excitation wavelengths were 488nm and 633nm. Fluorescent images of pancreatic cancer cell lines treated with CD133-grafted Cy5.5/PFOB@P-HVs individually were obtained using a confocal laser scanning microscope (CLSM, LSM710, Carl Zeiss, Germany). Every result was repeated for three times.

In vitro Ultrasound Imaging

To evaluate the in vitro ultrasound imaging capability of nanovesicles, the in vitro ultrasound images together with corresponding average gray values of indicated ROI (region of interest) for 2 mL PBS control, P-HMs, PFOB@P-HVs (concentration of all samples is 10 mg/mL) packed in a rubber tubing under different modes (B mode, contrast and harmonic) with mechanical index 0.6, 0.07 and 0.7, respectively, were captured with Aplio 500 (Canon, Japan) by using a linear probe (18MHz). In order to quantitatively measure the static picture captured, the “average grey value” was recorded. Every result was repeated three times.

Establishment of Tumor-Bearing Mice Model

Female BALB/c nude mice aged 4–6 weeks and weighing 20 ± 2.0 g were obtained from Shanghai Slac Laboratory Animal Co. Ltd. (China). Mice were bred in SPF clean rooms with a standard protocol and approved by in the Experimental Animal Center of the Shanghai Jiaotong University Affiliated Sixth People's Hospital (Permit Number: SCXK2013-0016). All animal experiments complied with the guidelines of China Council on Animal Care and the protocol. BxPC-3 cell lines were utilized for the tumor-bearing nude mice model. The BALB/c nude mice were injected with 1×10^6 cells subcutaneously per mouse for lower left side of the back area. The tumor-bearing mice model was built after 4–5 weeks. When the tumor volume reached ~500 mm^3, the tumor-bearing mice could be subjected to subsequent in vivo experiments.

In vivo Fluorescence Imaging

The Cy5.5-labeled CD133-grafted Cy5.5/PFOB@P-HVs or Cy5.5-labeled IgG-grafted Cy5.5/PFOB@P-HVs solutions were injected into tumor-bearing nude mice (n = 5 per group) via the tail vein, and fluorescence images were subsequently captured at different temporal points using an animal in intravital fluorescence imaging system (IVIS Spectrum, PerkinElmer, USA). Twenty-four hours after injection, the mice were euthanized to harvest six organs, namely, the heart, liver, spleen, lungs, kidneys, and tumor to perform fluorescence imaging. The fluorescence of the mice and main organs was expressed in units of photons/s/cm^2/sr. The fluorescence images obtained were studied using the Living Image® 4.5.2 software (Xenogen, PerkinElmer, USA).

Meanwhile, in order to evaluate the blood circulation of CD133-grafted Cy5.5/PFOB@P-HVs and IgG-grafted Cy5.5/PFOB@P-HVs, the nanovesicles solution was injected into the tail vein for three nude BALB/c mice in each group. At different pre-determined time points, 20 μL of blood was collected from the mice and then withdrawn. The fluorescence intensity of each blood sample was measured using a Varioskan Flash multimode microreader. Every result was repeated three times.

In vivo Ultrasonic Imaging of CD133-Grafted Cy5.5/PFOB@P-HVs in Subcutaneous Pancreatic Cancer Tumor Xenografts

Tumor-bearing nude mice were separated into two groups. The control group was injected with IgG-grafted Cy5.5/PFOB@P-HVs solution. The treatment groups were injected with a CD133-grafted Cy5.5/PFOB@P-HVs solution individually (5 animals per group) after degasification. The mice were administered with anesthetization with 1% pentobarbital sodium through intraperitoneal injection.

A Toshiba Aplio 500 clinical imaging system was used in THI mode at a mechanical index of 1.6 for in vivo observation of the tumor ultrasound imaging efficacy of the targeted nanovesicle solutions. The machine parameters were adjusted to achieve homogenous brightness, a frame rate of 10 fps, a gain of 60, and a dynamic range of 60 dB. The CD133-grafted Cy5.5/PFOB@P-HVs or IgG-grafted Cy5.5/PFOB@P-HVs solution (200 μL) was injected intravenously through the tail vein. The ultrasonic images of the implantation were captured before injection and at 2, 4, 8, 12, 24, and 36 h post-injection. The ultrasonic images were analyzed using the image-pro plus 6.0 software. Every result was repeated three times.

Ex vivo Assessment of the PFOB Enhancement Efficacy of Nanovesicles for HIFU Irradiation

Ex vivo evaluation of the enhancement efficacy of nanovesicles for the HIFU irradiation experiment was performed using a transparent tissue-mimicking phantom consisting largely of polyacrylamide gel and bovine serum albumin (BSA, A7906, 7% w/v, Sigma Aldrich UK, Dorset, 205 UK). The phantom was finished by mixing degassed and deionized water (60% v/v) with 40% acrylamide/bis-acrylamide solution (30% 200 v/v, Sigma Aldrich, UK). Then, ammonium persulfate (APS) powder (0.84% v/v, Sigma Aldrich, UK) was mixed in deionized water with complete magnetic stirring to make a 10% APS solution (10% w/v). The solution was placed inside a vacuum pump for degassing. Next, BSA (7% w/v) was added to the above solution with complete magnetic stirring where it was required to be filtered to exclude impurity. Subsequently,

four group samples of PBS, P-HMs (10 mg/mL), PFOB@P-HVs (10 mg/mL), and CD133-grafted Cy5.5/PFOB@P-HVs groups (10 mg/mL) were separately added to the tissue-mimicking phantom before catalyst addition with the same dosage and then subjected to the ultrasound irradiation at 40 W for 10s. Lastly, the catalyst, TEMED (0.05% v/v, Sigma Aldrich, UK) was added. This final solution was then poured into 5×5×5 cm acrylic molds and left to solidify overnight. Finally, the above phantom was fixed in an acrylic fixing plate for HIFU irradiation. The BSA protein contained in the phantoms will undergo denaturation above 50°C and will turn from opaque to white. The area of the denaturation lesions in the phantoms was measured manually subsequently after HIFU irradiation. The corresponding fusion volumes in the tissue-mimicking phantom of every group were acquired using the following equation: $V = \pi \times L \times W^2/6$, as L and W refer to the length and width of the ablated lesion, respectively. Meanwhile, ultrasound imaging was used to monitor the change in the gray value of the target lesions. Every result was repeated three times.

In vivo HIFU Therapy Using CD133-Grafted Cy5.5/PFOB@P-HVs in Tumor Xenografts

Four groups of nude mice bearing the tumor (n = 5 each group) were divided into five groups: saline, CD133-grafted Cy5.5/PFOB@P-HVs (10 mg/mL), saline + HIFU, IgG-grafted Cy5.5/PFOB@P-HVs (10 mg/mL)+HIFU, and CD133-grafted Cy5.5/PFOB@P-HVs (10 mg/mL)+HIFU. Meanwhile, the tumor areas were monitored using a B-mode pattern modality. Twenty-four hours after the intravenous injection, focused ultrasound was centered on the echo-enhanced site of the implantation at 40 W for 10s for the HIFU irradiation groups (T_{ON} = 1000 ms, T_{OFF} = 5000 ms), while the first group was left untreated as a control group. The tumor size was calculated using the following formula: $V = \pi \times \text{width}^2 \times \text{length}/6$. The corresponding pre-gray and post-gray scale values were documented and analyzed using the image-pro plus 6.0 analysis software. Subsequently, the cutoff tumor sections were acquired and stained with HE and TTC to distinctly observe the ablation area for histopathological analysis using an optical microscope. Every result was repeated three times.

Statistical Analysis

The research data were analyzed using SPSS 27.0 software. All quantitative information were showed as mean ± standard deviation. Differences between groups were assessed using analysis of variance (ANOVA). A p-value of <0.05 was considered to indicate a statistically significant difference.

Results and Discussion

Characterization

The CLSM image shows that the nanovesicles are equally distributed (Figure 1A) and fluorescently labeled (Figure 1C), while the SEM shows that the morphology is generally orbicular with a regular form (Figure 1B). The TEM image clearly demonstrated that the nanovesicles possess a dark PFOB core (Figure 1D), a gray organic/inorganic hybrid layer, and a diameter of approximately 100 nm. Furthermore, to observe the stability, nanovesicles were dispersed in PBS for 14 days, but no significant size change was observed (Figure 1E). The as-prepared solution remained stable for the 14 day period, and zeta analysis was used to the evaluate colloidal stability. After PEGylation, the zeta potential changed from –20.8 ± 0.6 mV to –3.2 ± 0.4 mV, which means that the PEG molecules were successfully grafted on the surface of the nanovesicles. Dynamic light scattering (DLS) was used to verify the size distribution. Thermogravimetric (TG) analysis was performed to affirm the being of PFOB in nanovesicles, and the PFOB loading rate of the nanovesicles was calculated to be 6.3 wt% (Figure 1F). The detection of -SH, Si-O-Si bonds and –COOH groups in the Fourier-transform infrared (FT-IR) spectra indicates that organosilica was successfully linked to the vesicle surface and that the CD133 antibody was successfully connected, respectively (Figure 1G). Energy dispersive X-ray spectroscopic (EDS) analysis further indicates the presence of Si, O, F, C, and S in the nanovesicles (Figure 1H). The emission wavelength of the CD133 and IgG-grafted Cy5.5/PFOB@P-HVs after synthesis was 710 nm. After HIFU irradiation, TEM made for displaying the morphologic change of the nanovesicles. As shown in Figure 1I and 1J, the nanovesicles became swollen and ruptured after HIFU irradiation at 10W for 5 min compared to the original nanovesicles.

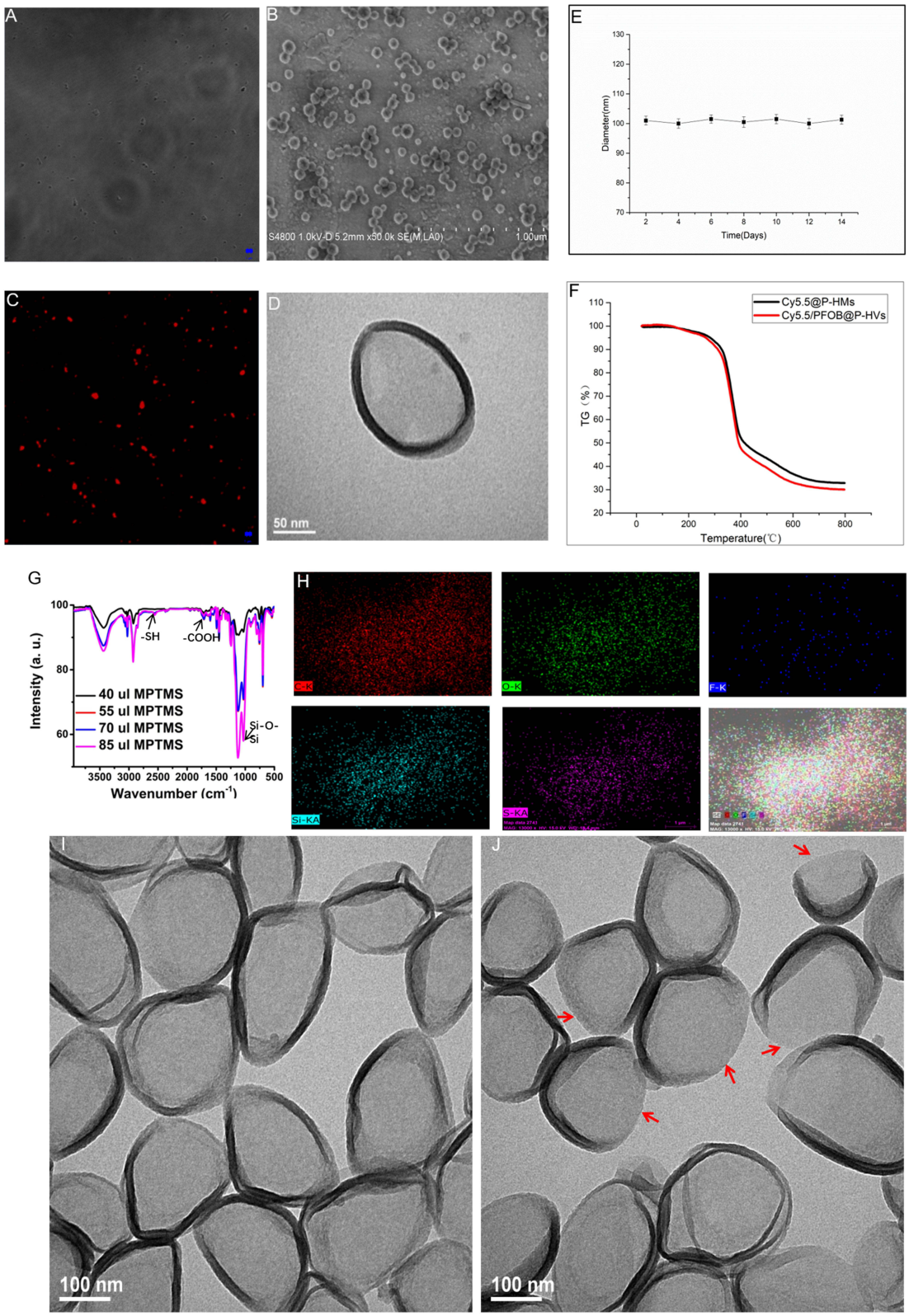

Figure 1 Manifestation of PFOB@P-HVs. (**A**) Optical microscope. (**B**) SEM image. (**C**) Confocal laser scanning microscopy (**D**) TEM image. (**E**) Size distribution of PFOB@P-HVs in PBS with time tested by DLS. (**F**) PFOB encapsulation rate measured by thermogravimetric analysis. (**G**) FT-IR. (**H**) EDS element mapping results of PFOB@P-HVs. (**I**) Nanovesicles morphology before HIFU irradiation. (**J**) Nanovesicles swollen and ruptured after HIFU stimulation. Red arrowhead: the margin of the ruptured shell.

In vitro Cytotoxicity and in vivo Biosafety

Before in vivo HIFU irradiation, an in vitro experiment was conducted to evaluate the ability of HIFU plus CD133-grafted Cy5.5/PFOB@P-HVs in killing pancreatic cancer cells. As shown in Figure 2A and B, the lethality of HIFU plus CD133-grafted Cy5.5/PFOB@P-HVs against BxPC-3 cells was improved by increasing the nanovesicle doses, and 95% of the BxPC-3 cells were killed when the nanovesicle concentration was increased to 20 mg/mL. For the CD133-grafted Cy5.5/PFOB@P-HVs group and IgG-grafted Cy5.5/PFOB@P-HVs group, the cell viability decreased slightly as the nanovesicle concentration increased, mainly due to osmotic injury at high concentrations. The cell viability for the CD133-grafted Cy5.5/PFOB@P-HVs plus HIFU group is lower than that for the IgG-grafted Cy5.5/PFOB@P-HVs plus HIFU group at different concentrations.

The viability of human BxPC-3 cells treated with different concentrations of CD133-grafted Cy5.5/PFOB@P-HVs for 24 and 48 h is shown in Figure 2A and 2B. As the concentration increased, the cell viability decreased slightly, but remained close to 90% at a concentration of 20 mg/mL (Figure 2A and B). After HIFU irradiation, the in vitro survival rate is as low as nearly 5%. During treatment, neglectable variation of body weight is found (Figure 2C). Blood routine indexes were also not significantly different among five groups (Figure 2D and E). Tissue sections of main organs stained with H&E showed no abnormal pathological changes (Figure 2F).

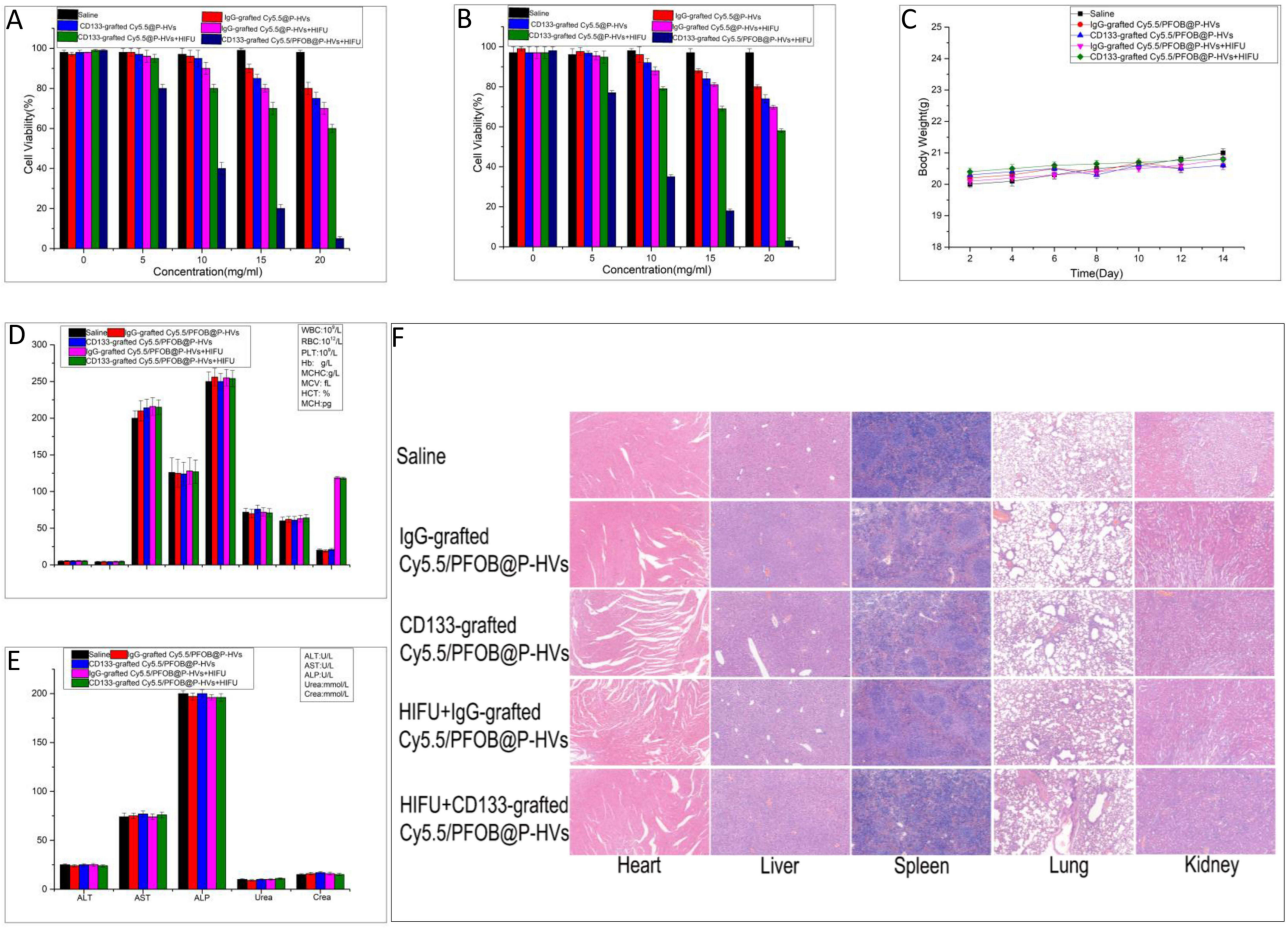

Figure 2 In vitro cytotoxicity and biosafety. Cell viabilities of BxPC-3 cells after co-culture with six groups individually with varied concentrations for 24 h (**A**) and 48 h (**B**), respectively. Data are expressed mean ± SD (n=5). (**C**) Time-related body weight change of the five groups. (**D**) Blood routine indexes analysis of mice after intravenously injection of with five groups individually. Data are expressed mean ± SD (n=5). Blood routine examination results: White blood cells (WBC) counts, Red blood cells (RBC) counts, Hemoglobin (HGB) counts, Hematocrit (HCT) counts, Mean corpuscular volume (MCV) counts, Mean corpuscular hemoglobin (MCH) counts, Mean corpuscular hemoglobin concentration (MCHC) counts, and Platelet (PLT) counts. (**E**) Hepatic and renal function indicator analysis of five groups at the end of treatments. Serum biochemistry data including Aspartate aminotransferase (AST), Alanine aminotransferase (ALT), and Alkaline phosphatase (ALP), Urea and Crea(creatinine). (**F**) H&E staining of main organs harvested from tumor-bearing mice after different corresponding treatments in five groups respectively. Scale bar:100μm.

Flow Cytometry Analysis

To compare the CD133 expression ratio on the cell surface in three human pancreatic cancer cell lines, flow cytometry analysis was performed (Figure 3A). CD133 expression was confirmed in all pancreatic carcinoma cell lines with different ratios. For the BxPC-3 cell line, the expression ratio was the highest at 0.98% ± 0.03%, while the expression ratios for PANC-1 and SW1990 were 0.69% ± 0.02% and 0.58% ± 0.05%, respectively. After repeating flow cytometry analysis more than thrice, the expression of CD133 protein on the cell surface among the three cell lines was found to be the highest for BxPC-3 cell lines, which paves the way for subsequent targeting experiments.

In vitro Targeting Experiment

To discuss the in vitro targeting ability of CD133-targeted nanovesicles with CD133-positive BxPC-3 cells, MACS was carried out to separate the CD133-positive and CD133-negative pancreatic cancer cells from among the general BxPC-3 cell lines. As shown in Figure 3B, the CD133-positive CSCs look spherical and suspended growing. After culturing for 2 h, the CD133-positive cells (DAPI: blue nucleus) were surrounded with Cy5.5-labeled targeted nanovesicles, while the CD133-negative cells were isolated with no surrounding Cy5.5-labeled-targeted nanovesicles. Above all, it is obvious that CD133-targeted nanovesicles are capable of combining CD133 positive CSCs specifically.

In vitro Ultrasonic Imaging Results

To assess the in vitro ultrasonic image capabilities of different composition of nanovesicles, three ultrasound mode of different nanovesicles were administered. Figure 3C shows that ultrasound images of three modes with significantly contrast agents under each modality were documented for PFOB@P-HVs groups, compared with P-HMs and the PBS control groups. Quantitative analysis reveals that the gray value P-PFOB@OIHVs groups is 3 times of P-HMs group in B mode, and twice of P-HMs group in harmonic and contrast mode, as shown in Figure 3D. In vitro ultrasonic imaging performance endowed the PFOB@P-HVs with ultrasonic (US) imaging properties. It indicated that PFOB@P-HVs groups are also capable of contrast agents comparing with the other two groups.

In vivo Fluorescence Imaging

To evaluate the blood circulation profiles of IgG-grafted Cy5.5/PFOB@P-HVs and CD133-grafted Cy5.5/PFOB@P-HVs, Figure 4C shows no difference. In order to monitor the targeting ability of CD133-grafted Cy5.5/PFOB@P-HVs in vivo, fluorescence imaging was conducted in subdermal pancreatic tumors. When the subcutaneous tumor achieved ~500 mm^3 in size, all mice were intravenously injected with IgG-grafted Cy5.5/PFOB@P-HVs or CD133-grafted Cy5.5/PFOB@P-HVs solutions. Fluorescence images were obtained from an IVIS fluorescence imaging system. Figure 4A shows that the fluorescence signal of the non-targeted group was observed throughout the whole body, but was more prominent in the tumor area after 8 hours post-injection. The solution was gradually metabolized and the fluorescence signal of tumor completely disappeared 12 hours after injection. In comparison, the fluorescence signal of the subcutaneous tumor region increased over time in the CD133-grafted Cy5.5/PFOB@P-HVs group, and achieved the maximum fluorescence accumulation at 24 h after injection. In vivo fluorescence imaging further demonstrated that CD133 modification improved the fluorescence accumulation of the CD133-grafted Cy5.5/PFOB@P-HVs. Comparing to that of the IgG-grafted Cy5.5/PFOB@P-HVs group at tumor site, as the qualitative analysis showed in Figure 4B. In vitro fluorescence results of tumors and main organs at 24 h after injection are shown in Figure 4D and E. In the IgG-grafted Cy5.5/PFOB@P-HVs group, fluorescence was gathered mainly in kidney and liver, with little enrichment at the tumor region. A higher signal was found at the tumor area for the CD133-grafted Cy5.5/PFOB@P-HVs-treated array.

In vivo Ultrasonic Imaging

The peak enhancement images of tumor ultrasonic imaging are displayed in Figure 4F. The information reveals that signal increased gradually, accordant with the results of intravital fluorescence results. To quantitatively evaluate the gray value of the ultrasound images, the image-pro plus 6.0 analysis software was used for analyzing the region of interest (Figure 4G). From 0 to 24 h after injection, the gray value of the tumor increased in the CD133-grafted Cy5.5/PFOB@P-HVs group and

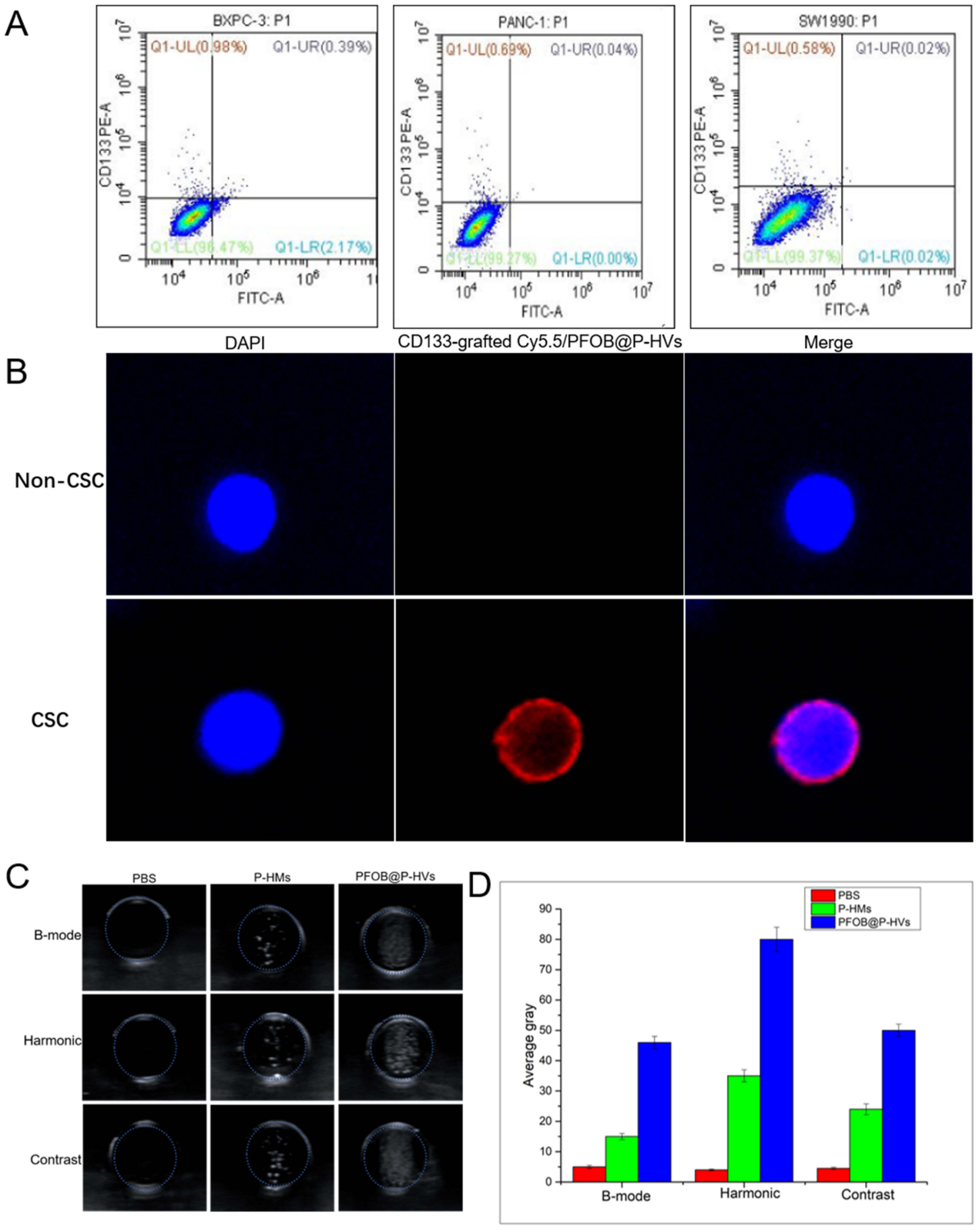

Figure 3 Flow cytometry analysis, in vitro targeting and in vitro ultrasonic imaging experiment. (**A**) Flow cytometry analysis. (**B**) In vitro targeting experiment.(blue: cell nucleus, red: Cy5.5-labeled nanovesicles). (**C**) In vitro ultrasonic imaging and (**D**) Quantitative analysis (blue circle area: region of interest).

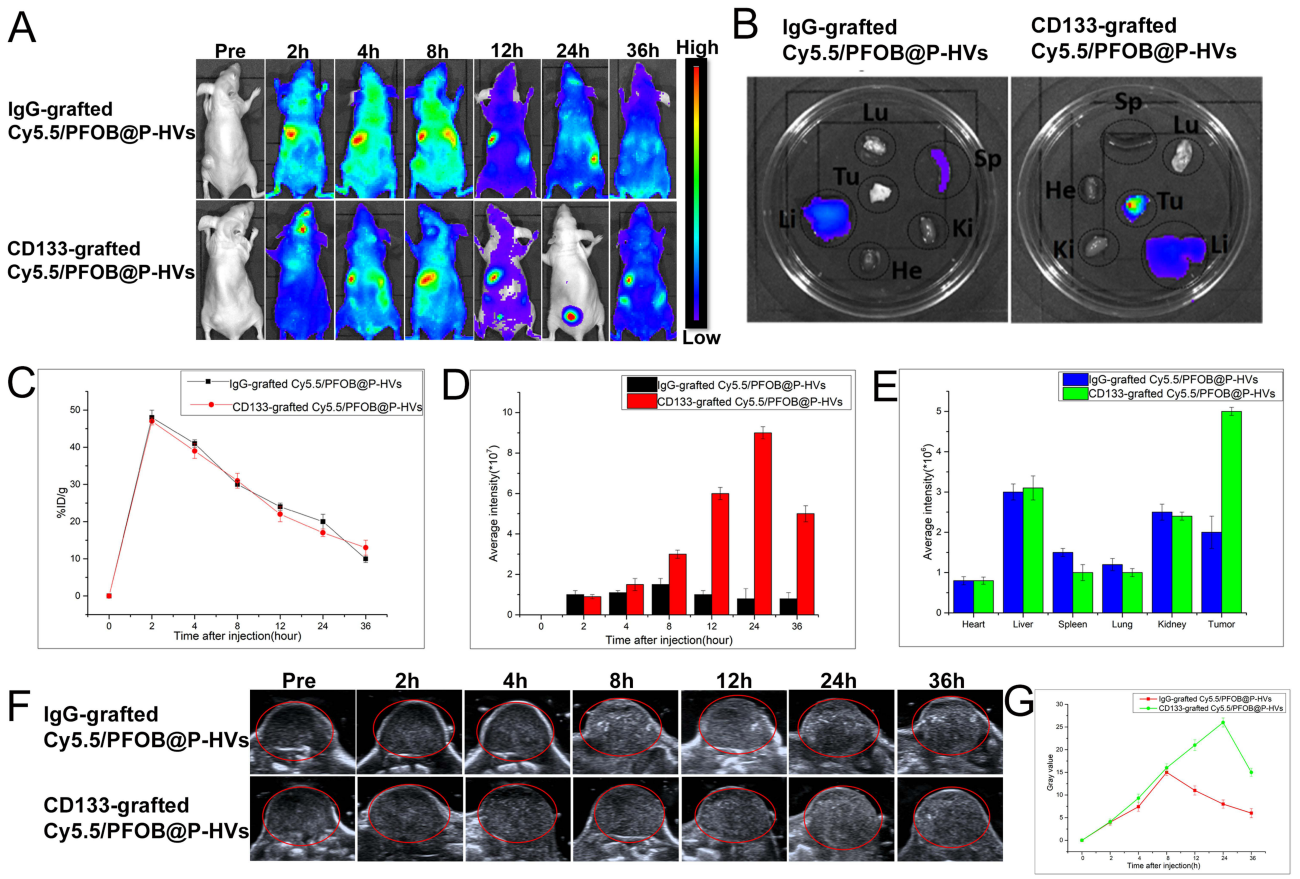

Figure 4 In vivo fluorescence imaging. (**A**) FL imaging of mice bearing BxPC-3 tumors 0h, 2h, 4h, 8h, 12h, 24h and 36h after intravenous injection of IgG-grafted Cy5.5/PFOB@P-HVs and CD133-grafted Cy5.5/PFOB@P-HVs solution. (**B**) Ex vivo FL imaging of tumors and main organs (liver, heart, spleen, lung, kidney) after 24h of administration. (**C**) In vivo blood circulation. (**D**) Quantitative analysis of fluorescence value of tumor with time post-injection. (**E**) Quantitative analysis of fluorescence value of tumors and main organs (liver, heart, spleen, lung, kidney) after 24h of administration. (**F**) In vivo ultrasonic imaging (red circle: region of interest). (**G**) Quantitative analysis of the gray value change for IgG-grafted Cy5.5/PFOB@P-HVs and CD133-grafted Cy5.5/PFOB@P-HVs.n=3.

came up to the peak level at 24 h after injection before gradually reducing ($p < 0.005$). However, for the IgG-grafted Cy5.5/PFOB@P-HVs group, the gray value increased until 8 h post-injection before reaching the peak, and then reduced gradually.

Ex vivo Phantom Irradiation Using HIFU

After HIFU irradiation, the gray scale and irradiation areas of the targeted region in different groups changed, as shown in Figure 5A. The ablation shape was irregular with a demarcated shape, and the gray scale of the focused area increased after HIFU treatment. The gray-scale changes were analyzed using the image-pro plus 6.0 analysis software. The gray scale changed from 50 to 53, 60 to 66, 58 to 80, and 62 to 90 for the PBS, P-HMs, PFOB@P-HVs, and CD133-grafted Cy5.5/PFOB@P-HVs groups, respectively. Statistical analysis showed that the difference was significant ($p < 0.01$). Subsequently, the gray scale change area in the phantom was measured in order to calculate the area using the following formula: $V = \pi \times L \times W^2/6 (mm^3)$. For the above four groups, the ablation area was calculated as 1.0 ± 0.1, 10.6 ± 0.3, 57.2 ± 0.5, and 105.5 ± 1.3 mm^3, respectively. The ablation area of the HIFU + CD133-grafted Cy5.5/PFOB@P-HVs group was statistically notably larger than that of the other three arrays ($p < 0.05$).

In vivo HIFU Therapy

The therapeutic efficacy of HIFU synergistic treatment combined with CD133-grafted Cy5.5/PFOB@P-HVs was evaluated on tumor-bearing nude mice. The results show that there was no statistical difference for the tumor size changes, HE and TUNEL staining results of saline group and CD133-grafted Cy5.5/PFOB@P-HVs group. After HIFU

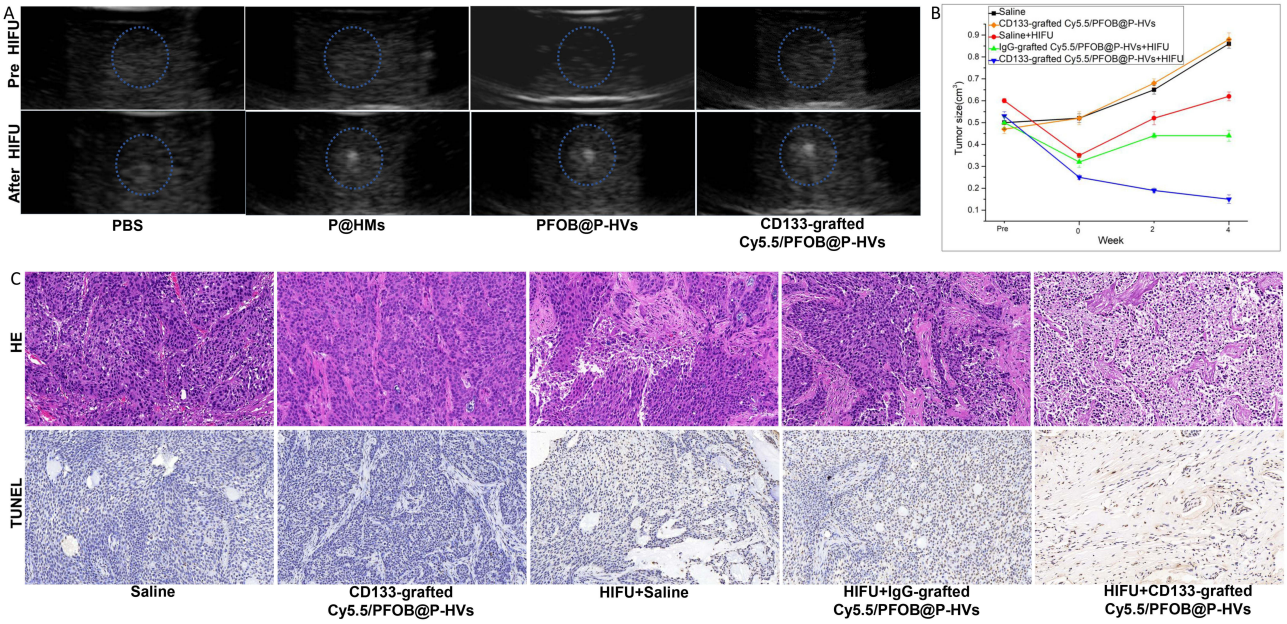

Figure 5 Ex vivo phantom HIFU irradiation and in vivo HIFU ablation experiment. (**A**) Ex vivo ultrasonic imaging of phantom after HIFU irradiation. (**B**) Tumor volume changes. (**C**) H&E and TUNEL staining for tumor after treatment. Scale bar:50μm.

irradiation, the subcutaneous transplantation turned from red to pale instantly in IgG-grafted Cy5.5/PFOB@P-HVs+ HIFU and CD133-grafted Cy5.5/PFOB@P-HVs +HIFU group, indicating tumor necrosis. Two weeks later, for the CD133-grafted Cy5.5/PFOB@P-HVs +HIFU group, the tumor had crusted over its surface completely, indicating repair of the necrotic tissue. However, for the IgG-grafted Cy5.5/PFOB@P-HVs+HIFU group, the subcutaneous tumor had crusted over only partially, and the tumor kept growing in part of the region, indicating residual revival of the tumor tissue. Three weeks later, the scab gradually became smaller in the CD133-grafted Cy5.5/PFOB@P-HVs +HIFU group. Meanwhile, for IgG-grafted Cy5.5/PFOB@P-HVs + HIFU group, the subcutaneous tumor kept growing, although it was smaller than that in the saline group. As shown in Figure 5B, the tumor volume changes were recorded and compared among the groups, and the HIFU + CD133-grafted Cy5.5/PFOB@P-HVs group tumor showed the largest volume change. H&E and TUNEL staining demonstrated that the CD133-grafted Cy5.5/PFOB@P-HVs + HIFU group could produce a larger area of necrosis than the other four groups (Figure 5C).

Conclusion

Our study demonstrated that HIFU combined with CD133 targeted therapy is effective and efficient for enhancing antitumor efficacy. The synthetic process is facile and nontoxic. The in vitro experiments showed that the constructed nanovesicles had a spheroidal structure with encapsulated PFOB and outward CD133 antibody modification. Meanwhile, the CD133-grafted Cy5.5/PFOB@P-HVs are targeted nanovesicles for CD133-positive pancreatic CSCs. The in vivo experiments demonstrated that CD133-grafted Cy5.5/PFOB@P-HVs with specific targeting characteristics exhibited dual-modal imaging ability and HIFU synergistic efficacy towards CD133-positive subpopulations.

Moreover, the assembly could be used for the diagnosis and treatment of pancreatic cancer and may have clinical applications in the future. Our study provides a potential treatment method for the patients with pancreatic cancer. As known, pancreatic cancer progresses rapidly with a poor prognosis, especially for cases that cannot be resected surgically. Despite the latest advances in chemotherapy and radiotherapy, it is still necessary to explore new therapeutic means with significant efficacy and less adverse effects. As reported, CSCs contributed to chemotherapy resistance. The recession of CD133 positive CSCs improve the sensitivity of chemotherapy. In conclusion, CSCs targeted nanovesicles combined with HIFU treatment may be a novel and promising therapy way for pancreatic cancer in clinical applications.

Acknowledgment

This work was supported by the National Natural Science Foundation of China (82171936).

Disclosure

The authors report no conflicts of interest in this work.

References

1. Siegel RL, Miller KD, Fuchs HE, Jemal A. Cancer statistics, 2021. *CA Cancer J Clin*. 2021;71(1):7–33. doi:10.3322/caac.21654
2. Fitzgerald TL, McCubrey JA. Pancreatic cancer stem cells: association with cell surface markers, prognosis, resistance, metastasis and treatment. *Adv Biol Regul*. 2014;56:45–50. doi:10.1016/j.jbior.2014.05.001
3. Rahib L, Smith BD, Aizenberg R, Rosenzweig AB, Fleshman JM, Matrisian LM. Projecting cancer incidence and deaths to 2030: the unexpected burden of thyroid, liver, and pancreas cancers in the United States. *Cancer Res*. 2014;74(11):2913–2921. doi:10.1158/0008-5472.CAN-14-0155
4. Ortiz-Sanchez E. Cancer stem cells in solid tumors. *Curr Stem Cell Res Ther*. 2019;14(5):374. doi:10.2174/1574888X1405190520103520
5. Adikrisna R, Tanaka S, Muramatsu S, et al. Identification of pancreatic cancer stem cells and selective toxicity of chemotherapeutic agents. *Gastroenterology*. 2012;143(1):234–45 e7. doi:10.1053/j.gastro.2012.03.054
6. Hermann PC, Huber SL, Herrler T, et al. Distinct populations of cancer stem cells determine tumor growth and metastatic activity in human pancreatic cancer. *Cell Stem Cell*. 2007;1(3):313–323. doi:10.1016/j.stem.2007.06.002
7. Olempska M, Eisenach PA, Ammerpohl O, Ungefroren H, Fandrich F, Kalthoff H. Detection of tumor stem cell markers in pancreatic carcinoma cell lines. *Hepatobiliary Pancreat Dis Int*. 2007;6(1):92–97.
8. Gallacher L, Murdoch B, Wu DM, Karanu FN, Keeney M, Bhatia M. Isolation and characterization of human CD34(-)Lin(-) and CD34(+)Lin(-) hematopoietic stem cells using cell surface markers AC133 and CD7. *Blood*. 2000;95(9):2813–2820. doi:10.1182/blood.V95.9.2813.009k20_2813_2820
9. Peichev M, Naiyer AJ, Pereira D, et al. Expression of VEGFR-2 and AC133 by circulating human CD34(+) cells identifies a population of functional endothelial precursors. *Blood*. 2000;95(3):952–958. doi:10.1182/blood.V95.3.952.003k27_952_958
10. Torrente Y, Belicchi M, Sampaolesi M, et al. Human circulating AC133(+) stem cells restore dystrophin expression and ameliorate function in dystrophic skeletal muscle. *J Clin Invest*. 2004;114(2):182–195. doi:10.1172/JCI20325
11. Singh SK, Hawkins C, Clarke ID, et al. Identification of human brain tumour initiating cells. *Nature*. 2004;432(7015):396–401. doi:10.1038/nature03128
12. Meyer MJ, Fleming JM, Lin AF, Hussnain SA, Ginsburg E, Vonderhaar BK. CD44posCD49fhiCD133/2hi defines xenograft-initiating cells in estrogen receptor-negative breast cancer. *Cancer Res*. 2010;70(11):4624–4633. doi:10.1158/0008-5472.CAN-09-3619
13. O'Brien CA, Pollett A, Gallinger S, Dick JE. A human colon cancer cell capable of initiating tumour growth in immunodeficient mice. *Nature*. 2007;445(7123):106–110. doi:10.1038/nature05372
14. Ricci-Vitiani L, Lombardi DG, Pilozzi E, et al. Identification and expansion of human colon-cancer-initiating cells. *Nature*. 2007;445(7123):111–115. doi:10.1038/nature05384
15. Yin S, Li J, Hu C, et al. CD133 positive hepatocellular carcinoma cells possess high capacity for tumorigenicity. *Int J Cancer*. 2007;120(7):1444–1450. doi:10.1002/ijc.22476
16. Suetsugu A, Nagaki M, Aoki H, Motohashi T, Kunisada T, Moriwaki H. Characterization of CD133+ hepatocellular carcinoma cells as cancer stem/progenitor cells. *Biochem Biophys Res Commun*. 2006;351(4):820–824. doi:10.1016/j.bbrc.2006.10.128
17. Collins AT, Berry PA, Hyde C, Stower MJ, Maitland NJ. Prospective identification of tumorigenic prostate cancer stem cells. *Cancer Res*. 2005;65(23):10946–10951. doi:10.1158/0008-5472.CAN-05-2018
18. Singh SK, Clarke ID, Terasaki M, et al. Identification of a cancer stem cell in human brain tumors. *Cancer Res*. 2003;63(18):5821–5828.
19. van Mackelenbergh MG, Stroes CI, Spijker R, et al. Clinical trials targeting the stroma in pancreatic cancer: a systematic review and meta-analysis. *Cancers*. 2019;11(5):588. doi:10.3390/cancers11050588
20. Swaminathan SK, Roger E, Toti U, Niu L, Ohlfest JR, Panyam J. CD133-targeted paclitaxel delivery inhibits local tumor recurrence in a mouse model of breast cancer. *J Control Release*. 2013;171(3):280–287. doi:10.1016/j.jconrel.2013.07.014
21. Yin W, Pham CV, Wang T, et al. Inhibition of autophagy promotes the elimination of liver cancer stem cells by CD133 aptamer-targeted delivery of doxorubicin. *Biomolecules*. 2022;12(11):1623. doi:10.3390/biom12111623
22. Tsai PH, Wang ML, Chang JH, et al. Dual delivery of HNF4alpha and cisplatin by mesoporous silica nanoparticles inhibits cancer pluripotency and tumorigenicity in hepatoma-derived CD133-expressing stem cells. *ACS Appl Mater Interfaces*. 2019;11(22):19808–19818. doi:10.1021/acsami.9b04474
23. Jiang J, Chen H, Yu C, et al. The promotion of salinomycin delivery to hepatocellular carcinoma cells through EGFR and CD133 aptamers conjugation by PLGA nanoparticles. *Nanomedicine*. 2015;10(12):1863–1879. doi:10.2217/nnm.15.43
24. Tan H, Hou N, Liu Y, et al. CD133 antibody targeted delivery of gold nanostars loading IR820 and docetaxel for multimodal imaging and near-infrared photodynamic/photothermal/chemotherapy against castration resistant prostate cancer. *Nanomedicine*. 2020;27:102192. doi:10.1016/j.nano.2020.102192
25. Wang X, Lu P, Zhu L, et al. Anti-CD133 antibody-targeted therapeutic immunomagnetic albumin microbeads loaded with vincristine-assisted to enhance anti-glioblastoma treatment. *Mol Pharm*. 2019;16(11):4582–4593. doi:10.1021/acs.molpharmaceut.9b00704
26. Cho JH, Kim AR, Kim SH, Lee SJ, Chung H, Yoon MY. Development of a novel imaging agent using peptide-coated gold nanoparticles toward brain glioma stem cell marker CD133. *Acta Biomater*. 2017;47:182–192. doi:10.1016/j.actbio.2016.10.009
27. Chen Y, Chen H, Shi J. Nanobiotechnology promotes noninvasive high-intensity focused ultrasound cancer surgery. *Adv Healthc Mater*. 2015;4(1):158–165. doi:10.1002/adhm.201400127
28. Ge HY, Miao LY, Xiong LL, et al. High-intensity focused ultrasound treatment of late-stage pancreatic body carcinoma: optimal tumor depth for safe ablation. *Ultrasound Med Biol*. 2014;40(5):947–955. doi:10.1016/j.ultrasmedbio.2013.11.020
29. Chen YL, Wang CY, Yang FY, et al. Synergistic effects of glycated chitosan with high-intensity focused ultrasound on suppression of metastases in a syngeneic breast tumor model. *Cell Death Dis*. 2014;5:e1178. doi:10.1038/cddis.2014.159
30. Sequeiros RB, Joronen K, Komar G, Koskinen SK. High intensity focused ultrasound (HIFU) in tumor therapy. *Duodecim*. 2017;133(2):143–149.

31. Khaibullina A, Jang BS, Sun H, et al. Pulsed high-intensity focused ultrasound enhances uptake of radiolabeled monoclonal antibody to human epidermoid tumor in nude mice. *J Nucl Med*. 2008;49(2):295–302. doi:10.2967/jnumed.107.046888
32. Li H, Yu C, Zhang J, et al. pH-sensitive pullulan-doxorubicin nanoparticles loaded with 1,1,2-trichlorotrifluoroethane as a novel synergist for high intensity focused ultrasound mediated tumor ablation. *Int J Pharm*. 2019;556:226–235. doi:10.1016/j.ijpharm.2018.12.006
33. Ma X, Yao M, Shi J, et al. High intensity focused ultrasound-responsive and ultrastable cerasomal perfluorocarbon nanodroplets for alleviating tumor multidrug resistance and epithelial-mesenchymal transition. *ACS Nano*. 2020;14(11):15904–15918. doi:10.1021/acsnano.0c07287
34. Shin SH, Park EJ, Min C, et al. Tracking perfluorocarbon nanoemulsion delivery by (19)F MRI for precise high intensity focused ultrasound tumor ablation. *Theranostics*. 2017;7(3):562–572. doi:10.7150/thno.16895
35. Niu D, Wang X, Li Y, et al. Facile synthesis of magnetite/perfluorocarbon co-loaded organic/inorganic hybrid vesicles for dual-modality ultrasound/magnetic resonance imaging and imaging-guided high-intensity focused ultrasound ablation. *Adv Mater*. 2013;25(19):2686–2692. doi:10.1002/adma.201204316
36. Pajek D, Burgess A, Huang Y, Hynynen K. High-intensity focused ultrasound sonothrombolysis: the use of perfluorocarbon droplets to achieve clot lysis at reduced acoustic power. *Ultrasound Med Biol*. 2014;40(9):2151–2161. doi:10.1016/j.ultrasmedbio.2014.03.026
37. Phillips LC, Puett C, Sheeran PS, Wilson Miller G, Matsunaga TO, Dayton PA. Phase-shift perfluorocarbon agents enhance high intensity focused ultrasound thermal delivery with reduced near-field heating. *J Acoust Soc Am*. 2013;134(2):1473–1482. doi:10.1121/1.4812866
38. You Y, Wang Z, Ran H, et al. Nanoparticle-enhanced synergistic HIFU ablation and transarterial chemoembolization for efficient cancer therapy. *Nanoscale*. 2016;8(7):4324–4339. doi:10.1039/C5NR08292G
39. Wang X, Chen H, Zhang K, et al. An intelligent nanotheranostic agent for targeting, redox-responsive ultrasound imaging, and imaging-guided high-intensity focused ultrasound synergistic therapy. *Small*. 2014;10(7):1403–1411. doi:10.1002/smll.201302846
40. Du M, Chen Y, Tu J, et al. Ultrasound responsive magnetic mesoporous silica nanoparticle-loaded microbubbles for efficient gene delivery. *ACS Biomater Sci Eng*. 2020;6(5):2904–2912. doi:10.1021/acsbiomaterials.0c00014
41. Kim S, Chen YS, Luke GP, Emelianov SY. In-vivo ultrasound and photoacoustic image- guided photothermal cancer therapy using silica-coated gold nanorods. *IEEE Trans Ultrason Ferroelectr Freq Control*. 2014;61(5):891–897. doi:10.1109/TUFFC.2014.2980
42. Wang X, Chen H, Chen Y, et al. Perfluorohexane-encapsulated mesoporous silica nanocapsules as enhancement agents for highly efficient high intensity focused ultrasound (HIFU). *Adv Mater*. 2012;24(6):785–791. doi:10.1002/adma.201104033
43. Wang X, Chen H, Zheng Y, et al. Au-nanoparticle coated mesoporous silica nanocapsule-based multifunctional platform for ultrasound mediated imaging, cytoclasis and tumor ablation. *Biomaterials*. 2013;34(8):2057–2068. doi:10.1016/j.biomaterials.2012.11.044
44. Zhou Y, Han X, Jing X, Chen Y. Construction of silica-based micro/nanoplatforms for ultrasound theranostic biomedicine. *Adv Healthc Mater*. 2017;6(18):1700646. doi:10.1002/adhm.201700646
45. Ma M, Xu H, Chen H, et al. A drug-perfluorocarbon nanoemulsion with an ultrathin silica coating for the synergistic effect of chemotherapy and ablation by high-intensity focused ultrasound. *Adv Mater*. 2014;26(43):7378–7385. doi:10.1002/adma.201402969
46. Liberman A, Wu Z, Barback CV, et al. Hollow iron-silica nanoshells for enhanced high intensity focused ultrasound. *J Surg Res*. 2014;190 (2):391–398. doi:10.1016/j.jss.2014.05.009
47. Rouffiac V, Duret JS, Peronneau P, et al. Combination of HIFU therapy with contrast-enhanced sonography for quantitative assessment of therapeutic efficiency on tumor grafted mice. *Ultrasound Med Biol*. 2006;32(5):729–740. doi:10.1016/j.ultrasmedbio.2006.02.1403
48. Kim JH, Kim H, Kim YJ, Lee JY, Han JK, Choi BI. Dynamic contrast-enhanced ultrasonographic (DCE-US) assessment of the early response after combined gemcitabine and HIFU with low-power treatment for the mouse xenograft model of human pancreatic cancer. *Eur Radiol*. 2014;24 (9):2059–2068. doi:10.1007/s00330-014-3260-4